

A HIGH DUTY FACTOR 400 MeV HIGH RESOLUTION ELECTRON LINEAR ACCELERATOR*

J. HAIMSON

*Massachusetts Institute of Technology
Cambridge, Massachusetts*

Introduction

An increasing need for electron beams of higher intensity, resolution, and duty factor, in high energy nuclear physics research, provided stimulus for the re-appraisal and extension of existing microwave accelerator concepts, and the investigation of alternate new techniques. Most of the high duty factor microwave electron accelerator projects presently being pursued in a number of laboratories throughout the world comprise either, (a) "conventional" linacs and microtrons, which utilize high power RF generators and high dissipation waveguides or (b) superconducting linacs and microtrons, which hold promise of eventually achieving the ultimate in high duty factor-high energy performance, namely, continuous operation. In the former category, system design concepts were previously limited due to the nonavailability of suitable high duty factor RF generators. In recent years, however, the reliable demonstration of very high levels of RF power over a range of different frequency bands enabled several high duty factor accelerator projects to be initiated. 1,2,3

The MIT electron linac described in this paper utilizes 2856 MHz klystrons which operate over a wide dynamic range of peak RF power from 4 MW to 1 MW with a corresponding average RF power range of 80 kW to 65 kW, i.e., a range of RF duty factors from 2 percent to 6.5 percent. High duty operation with this technique, however, imposes unusual technical and economic restrictions on the design of the linac because of the weak accelerating field strengths associated with the low values of peak RF power, and the uncommonly high levels of average

* Work supported by the U. S Atomic Energy Commission and the Massachusetts Institute of Technology.

power, that must be dissipated in the thermally phase sensitive and dispersive elements of the system, such as the accelerator sections and the rectangular waveguide feeds.

For example, in order to compensate for loss in energy gain due to the reduced field gradients there is a strong design tendency to maximize the length and total attenuation (τ) of the waveguide sections consistent with the requirements of phase and temperature stability ($\Delta\theta/\Delta f=2\tau Q/f$, $\Delta f/\Delta T=48$ kHz/°C). Also, the waveguides generally require water cooling systems which are designed to operate with large flows and high velocities, and which incorporate means for the accurate automatic temperature control of the phase shift through the section. In this regard, control of the inlet water temperature with a sensitive metal temperature detector located at a unique temperature—phase "fulcrum" point on the waveguide is found to be effective in maintaining a given phase relationship, regardless of variation of input RF power or beam loading.

Since, with a linac system of the above type, high duty performance is obtained by operating at a maximum repetition rate of several thousand pulses per second and pulse lengths in excess of 10 μ sec, it is clear that adjustment of these parameters can cause large variations of dissipated power throughout the system. A requirement that the RF and injection systems be designed for reliable and stable performance over very wide limits of pulse operation is characteristic of this high duty factor approach.

Quite apart from the principal advantage of increasing the beam intensity, high duty operation manifests another particularly valuable feature; namely, that despite inherently low field gradients, high duty factor linacs are subject to considerably less beam loading than conventional low duty high gradient machines of the same beam energy and average current. (For a given klystron and waveguide configuration and a constant average current the beam loading parameter is inversely proportional to the square root of the duty factor). This characteristic is instrumental in reducing several of the larger contributions to beam energy spread and is primarily responsible for the inherent capability of high duty factor linacs to produce electron beams of higher resolution than conventional duty machines.

A comprehensive description of system optimization and design procedures for high duty factor linacs has been given recently elsewhere,³ and the following discussion refers specifically to the 400 MeV linac currently under construction at the Laboratory for Nuclear Science, MIT, and performance data obtained during preliminary tests on several of the prototype sub-systems.

Design Objectives

In determining a suitable concept for the MIT linac, the study of various RF and beam optics problems established two important design objectives. The first was to elevate the threshold current level of the cumulative type of beam break-up (BBU) well above the normal operating levels of the machine, bearing in mind that high duty operation necessitated low field gradients and long pulse lengths — conditions which were known to be conducive to the BBU instability phenomenon. The second objective was to exploit as fully as possible (to the extent permitted by limited funds) the high duty factor capability of producing sharp spectra beams of high intensity. In this regard, design emphasis was placed on achieving input RF power and beam injection of high quality and on maintaining an accurate phase relationship and a central beam trajectory within each waveguide.

The design objectives for the three prime RF operating parameters, phase, field strength, and frequency were, respectively, <2 degrees of intrapulse phase variation (droop and ripple), with respect to the phase of the drive power, for pulses up to 15μ sec in length; $<\pm 0.125$ percent of intrapulse variation of the field gradient at the waveguide input couplers; and <1.5 kHz long term frequency variation of the master exciter. These RF objectives led to the choice of an ultrastable phase-locked solid state exciter, cw booster drive klystrons using 0.02 percent voltage regulated dc power supplies and pin-diode modulated RF input signals, direct HV series switching of the main klystrons (hard tube modulators) without the use of pulse transformers, and temperature-phase control of the critical RF systems.

Consistent with the inherent high resolution capability of a lightly loaded accelerator operating with pulses an order of magnitude longer than the fill-time of the waveguides, the injector design studies placed emphasis on the attainment of very narrow bunch widths. A 2 degree design objective was established for the longitudinal phase space of bunches emergent from the injector linac at energies greater than 6 MeV and for peak currents of up to 25 mA. Owing to space charge and waveguide space harmonic considerations³, the above requirements led to the choice of a high potential electron gun (maximum of 500 kV), an RF chopper prebuncher system, and a slightly tapered phase velocity buncher waveguide designed to operate at a high level of dissipation.

Choice of a high gun potential, a small cathode diameter, a long focal length, and the use of narrow collimating apertures, in combination with a low value of longitudinal phase space ($<10^\circ$) at injection to the buncher waveguide, held promise of demonstrating a considerably lower beam emittance than that previously obtained with higher perveance, lower potential, injection systems. These features were consistent also with the desire to inject and accelerate small cross-section beams and to maintain the trajectories as close as practicable to the central axis. To assist in this objective, two pairs of beam steering

Helmholtz coils are located at each waveguide section in close proximity to the RF input couplers, and solenoidal focusing has been provided for the first five waveguide sections with several quadrupole doublet assemblies thereafter.

General Description of Machine

A schematic layout of the microwave distribution system, the injector linac, and the accelerator waveguide arrangement is illustrated in Figure 1. Ten high power klystrons are paired into five groups, each pair being video driven from a common hard tube modulator and RF driven from a common driver klystron. A highly stabilized master driver klystron is used to excite the five driver klystrons via a phase stabilized coaxial line.

Ten rectangular waveguide networks are utilized to interconnect the high power klystrons to 24 accelerator waveguide sections. The first klystron is reserved for the two series-connected sections of the injector linac; each of the following seven klystrons drive two waveguide sections; and each of the last two klystrons energize four accelerator sections. The use of quadruplexed waveguide sections at the end of the linac provided a satisfactory compromise between the technical desire to maximize beam energy and the economic requirement to minimize initial expenditure. The approach has an added attraction in that the machine can be up rated at a later date, without affecting the beam centerline components, by adding another transmitter and retrofitting a portion of the RWG network in the gallery.

The 24 accelerator waveguide sections comprise a buncher in series with a 3.7 meter section, four 3.7 meter sections, and eighteen 7.35 meter sections. The accelerator waveguides are divided into six groups of different microwave design, shown in Figure 1 as AA, BB, A, B, C, and D, in order to (a) provide a higher gradient at the beginning of the linac and (b) counteract the cumulative type of BBU.

Description of Linac Characteristics

Principle Performance Specifications

Beam energy at zero loading	430 MeV at 1.8% duty
Beam energy at an average current of 150 mA	400 MeV at 18% duty
Energy spread at 150 mA average	> 50% current in $\pm 0.2\%$
Beam emittance at 400 MeV	2×10^{-6} rad \times cm

Main Features

Number of klystrons	10
Linac design operating frequency	$2856 \pm .05$ MHz
Number of modulators	5

Number of waveguide sections	24 ($2\pi/3$ design)
Overall electrical length	152 meter
Overall physical length	180 meter

Master Driver

Crystal controlled solid state oscillator

Frequency range (manual control)	2856 \pm 6 MHz
Vernier adjustment (electronic control)	\pm 150 kHz
Long term stability	1 part in 10^7
Power output (cw)	400 mW
Trigger logic controlled diode modulation	

Master driver klystron	Type 4K3SN-1
Power output (cm rating)	1 kW
Bandwidth (Output)	< 0.1 db variation for 2856 \pm 0.5MHz
Beam voltage	6.2 kV dc
Beam current	470 mA dc
Drive power (nominal)	75-150 mW
Electrical length	2240 degrees at 7 kV
Filament power	6.0 V dc x 4.8 A dc
Focus	Permanent magnet
Collector cooling	3 GPM at 23 psi
Body cooling	1 GPM at 6 psi

High Voltage power supply

Voltage range	0 - 8 kV dc
Current range	0 - 600 mA dc
Voltage ripple and regulation	$< \pm 0.01\%$
HV vernier control	0.03%

Main Drive Line

1 - 5/8 inch coaxial line	190 meter long
Group velocity	$0.98c < v_g < 1.02c$
Phase velocity	$> 0.997c$

Coaxial directional couplers	5 at 2W peak output 1 at 5W peak output
Coaxial expansion joints	4
Temperature control	$\frac{1}{2}^{\circ}\text{C}$
Pressure control (dry N ₂)	1/10 psi
Overall phase stability	1 degree
Driver Klystrons	5 (Type 4K3SN-1, as above)
HV dc power supplies	5 (as above)
Main Klystrons	10 (Type VA938)
Operating frequency	2856 \pm 0.2 MHz
Peak output RF power	4 MW to 1 MW
Peak beam voltage (max)	130 kV to 80 kV
Peak beam current	91 A to 44 A
Microperveance	2.0 \pm 0.1
Average output RF power	80 kW to 65 kW
Minimum efficiency	35% to 30%
Minimum gain for saturation	41 db
Maximum body current	3%
Filament power (max)	700 W
Focus	Electromagnetic (4 coils)
Collector cooling	75 GPM at 70 psi
Body and window cooling	10 GPM at 10 psi
Single RF output through ceramic window	
Window pressurization (dry N ₂)	50 psi (max)
Modulators (Hard Tube)	5 (Type ESI)
Peak Power	23 MW at 1.25 kHz, 7MW at 4 kHz
Average Power	520 kW
Peak voltage	140 kV
Peak current	200 A
Load dynamic impedance	1400 to 1700 ohm
Switch tubes	Four Litton - L5097 rated 165 kV
Capacitance bank	1.8 μF
Crowbar protection	Maximum energy release < 50 joule
Pulse duration (99% flat-top)	Continuously variable up to 15 μsec in accordance with duty factor and peak power (see Figure 4)

Voltage pulse flat-top specification	0.2% (objective 0.1%)
Pulse repetition rate	Continuously variable up to 5 kHz in accordance with duty factor and peak power (see Figure 4)
RF duty factor	2% to 6.5%
Video duty factor	2.5% to 8%

Main Waveguide Sections (4 short and 18 long)

$2\pi/3$ mode, approx. constant gradient.

Length

3.675 and 7.35 meter

Number of cavities

105 and 210

Circ thickness

5.84 and 5.84 mm

Number of uniform segments per section

11 and 11

Range of shunt impedance

53.8-57.7 and 48.0-56.5 M Ω /m

Range of group velocity (v_g/c)

0.0156-0.007 and 0.0389-0.0093

Average attenuation parameter

0.75 and 0.825 neper

Average Q

13400 and 13750

Filling time

1.12 and 1.27 μ sec

Zero current energy gain at $P_o = 1.8$ MW

16.6MeV and 23.2MeV

Zero current energy gain at $P_o = 0.8$ MW

15.5MeV

Cooling

12 \times 11 mm I.D. and 8 \times 16 mm I.D. tubes

Water flow per section

6.3 and 6.3 litre per sec.

Construction

Hydrogen braze (copper-silver eutectic) and vacuum jacket

Beam pulse length

Variable up to 14 μ sec in accordance with duty factor and peak RF power.

Beam duty factor

1.8% at $P_o = 4$ MW and 5.8% at $P_o = 1$ MW.

Steering coils at each input coupler, no solenoids for long sections.

Injector Linac Design

Electron gun maximum potential	500 kV
Nominal operating potential	400 kV
Nominal cathode current	100 mA
Mod electrode potential	2 to 5 kV (-500 V bias)
Chopper cavity	TE ₁₀₂ mode
Prebuncher cavity	TM ₀₁₀ mode
Drift length	1.3 meter
Injected bunch width	< 10 degrees
Buncher waveguide	Tapered phase velocity, 2 π /3 design, 1.2 meter long.
Series-connected waveguides	$v_p=c$, 2 π /3, 3.7 meter long
Buncher zero load energy	6.9 MeV at P _o =2.5 MW
Beam design emittance at 6 MeV	10 ⁻⁴ rad \times cm
Focus	Thin lenses and solenoids

RF System

At high duty factor, the provision of a reliable, phase stable RF drive system extending over the full length of the accelerator presents a severe design problem owing to the high levels of power dissipation. This problem can be avoided by the use of intermediate drive klystrons which are excited via a common coaxial line and a master RF driver as shown in Figure 1. The use of a rigid coaxial cable for a main drive line is highly desirable in a multi-klystron driven accelerator since the group velocity can be closely approximated to the velocity of light; and because of low dispersion characteristics, a coaxial cable is more tolerant to small changes of frequency and ambient temperature than a rectangular waveguide. On the other hand, unlike a rectangular waveguide, a coaxial line which is subject to wide variations and moderate levels of dissipation is difficult to phase stabilize owing to the inaccessibility of the center conductor. With the above technique, however, the drive line dissipation level remains low even at the maximum duty factor, and attention need only be directed at controlling the ambient environment. Another advantage of the coaxial line is that its geometry

readily allows the use of bellows type expansion joints, and by judicious location of these joints, it is possible to anchor the drive line at each of the directional coupler feed points. This allows the phase relationship between each of the driver klystron feed points to be spatially locked, and the telescoping action within each segment prevents the drive line from being seriously stressed.

While the use of driver klystrons offers several distinct advantages, especially the very low power rating permitted for many of the components, extreme care must be taken to avoid radiative feedback into what is essentially a long distributed high gain amplifier system. A potential source of interference is the RF leakage associated with isolated collector high power klystrons; and low-level drive line components such as couplers, flanges, etc. should be well shielded and/or remotely located in a shielded duct.

The RF master exciter consists of a tunable phase-locked crystal-controlled solid state oscillator which drives a water-cooled klystron. All phase-locked and oscillator components are oven-controlled for high stability, and pin-diode modulation capability of the 400 milliwatt oscillator output enables optional cw or pulsed operation of the klystron. The klystron is rated at 1 kW cw, requires a drive of 150 mW (nominal) and is energized by a remotely adjustable HV regulated dc power supply having a voltage ripple of less than 0.02 percent peak to peak. Power from the main 1-5/8 inch coaxial drive line is coupled out to excite the five 1 kW driver klystrons, each of which provides drive for two high power klystrons. With this approach, even at 10 percent duty, the total dissipation in the main drive line is limited to less than 70 watts, and the drop-out lines (2W peak) and components connecting to the driver klystrons operate at an average power of a few hundred milliwatts. The five driver klystrons are identical in design to the master driver klystron and are energized from similar highly stabilized dc power supplies. Thus, all driver klystrons operate with dc beams and derive pulsed input RF signals from a triggerlogic-controlled modulation of the master oscillator output. This drive system concept was chosen as the most likely to reliably provide a 1 degree phase stability for the main klystron drive signals as well as for the main drive line in its role as a master reference for phasing the accelerator.

Figure 2 shows the completed master driver cubicle (background) and a high precision phase bridge capable of resolving phase differences of less than 0.1 degree between signals connected to the two input arms of a carefully matched and balanced magic Tee. Typical phase performance data obtained during final tests on the master driver system are shown in Figures 3(a) and (b). These phase measurements were taken at 5000 pulses per second, with one arm of the bridge sampling the output of the solid state exciter and the other arm sampling the pulsed output of the driver klystron when operating at a peak power of 800 watts. Figure 3 (a) shows the flat phase characteristic obtained for

a pulse length of 33 μ sec. For calibration purposes, as shown in Figure 3(b), a 1 degree phase shift off-set is superimposed on the 33 μ sec pulse trace of the phase bridge output, i.e. the RF phase stability over the full length of the pulse flat top is <0.3 degrees. This RF flat-top phase stability has also been demonstrated over a wide range of repetition rates and with pulse lengths extending into the millisecond region, which is consistent with the cw beam operation of the driver klystron, a 1 volt peak to peak ripple of the HV power supply, and a klystron transit length of 2420 degrees at 6 kV. The long term (24 hours) frequency drift of the master driver unit is between 200 and 300 Hz, which is well within the operational requirements of the linac. It should be noted that the pin-diode presently being used to modulate the cw output of the exciter introduces a relatively large transient phase shift (~ 2 degrees) during initial switching, and a delay of approximately 6 μ sec is required before the steadystate condition is reached. Further development work is being planned to investigate this phenomenon.

The high power klystrons are of five cavity construction, each requiring a peak RF drive of approximately 50 watts and using a single waveguide output feed which is terminated in a half wavelength (solid block) water-cooled ceramic window. A short section of thick-wall, pressurized waveguide, terminated with a similar RF window, connects the klystron to the evacuated rectangular waveguide system. This section serves the dual role of providing additional cooling for the klystron window (average power 80 kw) and enabling klystron replacement without disturbing the vacuum system. It also provides a convenient location for the four directional couplers used for RF protection and monitoring purposes. The evacuated rectangular waveguide networks are similar to those used at SLAC, with the exception that an extra water cooling channel has been added to the high power sections between the klystrons and the power splitters. RF monitoring couplers are located on either side of the driver and main klystrons and in the rectangular waveguide feeds immediately prior to each accelerator waveguide input coupler. In order to minimize transverse momenta contributions to the beam, due to coupler asymmetries, the rectangular waveguides are arranged as vertical input feeds from above (A) and below (B) the accelerator structure in an ABBA BAAB ABBA BAAB BA BAAB configuration, as shown in Figure 1. To further cancel the effects of coupler asymmetry, the input and output RF feeds are located on the same side of each accelerator waveguide; and, to provide local correction, two pairs of beam steering Helmholtz coils are located at each input coupler. In keeping with a philosophy to avoid unnecessary evolution of gas within the vacuum system, especially during long pulse operation, the accelerator waveguide output feeds are connected to water loads which are isolated from the vacuum by two quarter wavelength ceramic windows separated by a short section of air-filled rectangular waveguide.

Again, this section serves the dual purpose of providing a convenient location for the output RF power monitor and avoiding a catastrophic situation in the event of a window failure. Since there are no high power phase shifters in the system, reliance is placed on the accurate determination and manufacture of the rectangular waveguide lengths, and on final tuning of the waveguides after installation, to provide correct phase relationships within individual networks.⁴

Prototype Transmitter Performance

Hard tube modulators and direct series switching were chosen for the MIT linac because of the need for high quality video pulses and a maximum repetition rate of 5000 pulses per second, and the desire to continuously vary the peak RF power and pulse length over the full dynamic range of the system. The operational limits of RF pulse width and repetition rate for the transmitter are related to the klystron peak RF power and permissible duty factor as indicated in Figure 4.

The absence of pulse transformers, made possible by the direct high voltage switching approach, enables pulse ripple and droop contributions due to leakage reactance and stray capacitance to be reduced to very low values. The prototype transmitter described below utilized two paralleled switch tubes in series connection with each klystron. These switch tubes use magnetron injection gun geometry, with the cathode well protected from arcs, and are of gridless construction. The high plate resistance of the two switch tubes in parallel (more than twenty times the dynamic impedance of the klystron) is an essential characteristic which provides the regulation necessary for meeting the jitter and drift specifications and allows economy in the capacitor banks.

Video and RF preliminary tests were conducted recently on the prototype transmitter using one klystron and two switch tubes. The results of these tests were particularly impressive, especially in regard to pulse quality and stability, and a summary of the performance data is given below.

The klystron was operated as a diode load for the video power tests, and the body current was carefully monitored and maintained at a low level throughout the test period. Continuous adjustment capability of the video peak power was demonstrated by operating at a variety of klystron beam conditions between 126 kV, 88.3 amps (11.1 MW) and 67 kV, 35 amps (2.3 MW) with a 16 μ sec flat-top pulse at 660 pps. High average video power tests were also conducted at both high and low peak power conditions, e.g., 10.9 MW peak at 1.9 percent flat-top duty (152 μ sec flat-top at 1250 pps), and 3.27 MW peak at 6.0 percent flat-top duty (15.6 μ sec flat top at 3850 pps). In addition, video pulse modulation, droop and jitter measurements were taken at peak power levels of 122 kV, 84 amps (10.3 MW), and 79 kV, 45 amps (3.5 MW).

The maximum observed intrapulse voltage amplitude modulation was <0.05 percent for both peak power conditions (Specification is 0.2 percent except during the first and last microsecond).

The droop in pulse current after 15μ sec was measured as <0.05 percent in the high peak power condition and 0.11 percent rise in the low peak power condition (specification is ≤ 0.5 percent).

Short term jitter pulse instabilities were measured over the range of permissible repetition rates at both the low and high peak power conditions. The voltage jitter was approximately 0.03 percent (specification is 0.17 percent) with occasional current pulse jitter values of about 0.05 percent (specification is 0.25 percent).

Figure 5 shows some of the prototype transmitter components including the dual capacitance bank, the crowbar protection assembly, the modulator tank with its HV bushing, and the tank containing the HV dc power supply. Figure 6 is a view of the interior of the modulator tank showing two of the switch tubes and a high power klystron.

The master driver described earlier, and shown in Figure 2, was used to excite the main klystron during the RF preliminary tests. The klystron output rectangular waveguide was pressurized with dry N_2 and instrumented for excess reverse power protection, arc protection, and forward power measurements, and was terminated in a matched water load calorimeter. Data obtained during these preliminary tests verified peak RF power outputs over the range of 4.4 MW to 0.75 MW. Full average RF power output was not attempted during the first series of tests, although the klystron was operated at up to 50 kW RF average, as efforts were concentrated on obtaining RF phase data during the pulse.

The diagnostic value of an accurate RF phase bridge cannot be over-emphasized since it provides a sensitive and easily calibrated means of qualitatively and quantitatively analyzing the performance of both the RF system and the modulator. By progressive comparison of pulse signals across the driver and main klystrons (or with the "standard" arm of the bridge connected to the cw source of RF power), the various phase modulation contributions due to RF drive, modulator pulse voltage droop and ripple, klystron cathode heater hum, temperature drift, etc., can be readily isolated and measured. The modulator intrapulse voltage amplitude variations can be determined essentially in time domain, thus avoiding the errors (and perennial debates) associated with high voltage monitor corrections factors (compensation of capacitance dividers, droop of monitoring pulse transformers, ringing, etc)—especially when the variations being considered are small fractions of one percent.

For example, the transit phase angle (Φ) through a klystron is related to the electron velocity (βc) and drift distance (S) between terminal cavity gaps by the simple expression, $\Phi = 2\pi S / (\beta \lambda_0)$. Differentiating this expression with respect to the klystron cathode voltage (V) gives, $(\partial \Phi / \partial V) = (\partial / \partial V) [2\pi S \gamma (\gamma^2 - 1)^{-\frac{1}{2}} / \lambda_0]$, where λ_0 is the free space wavelength, and the electron energy in rest mass units (γ) is given

by, $\gamma = 1 + V(\text{keV})/511 = 1/(1 - \beta^2)^{1/2}$. This then gives the relativistically corrected phase shift $[\Delta\Phi]$ through the klystron for small fluctuations of cathode voltage (ΔV) as, $\Delta\Phi = -(\Delta V/V) [2\pi S (\gamma - 1)(\gamma^2 - 1)^{-3/2} / \lambda_0]$. As an example, at a frequency of 2856 MHz and with a klystron drift distance of 35 cm, a cathode voltage variation of 0.1 percent will produce klystron phase variations of 0.73 and 0.96 degrees at cathode potentials of 122 kV and 80 kV, respectively. Additional cross-checks on the video performance, as determined from RF phase measurements, can be conducted by observing the associated intrapulse amplitude variation of the RF power and using the perveance relationship of a space charge limited beam, i. e., $(\Delta P/P) = (5/2) (\Delta V/V)$.

Typical RF phase pulse characteristics obtained during the preliminary tests are shown in Figures 7(a) and (b). Figure 7(a) was obtained with the phase bridge connected across the input of the driver klystron and the output of the main klystron, i. e., measuring the combined phase shift of both klystrons. For this example, the main klystron was operated at the low end of the peak power range (80 kV, 44.9 amps) and therefore at the highest phase sensitivity, due to the low cathode potential. The trace shows a phase **advance** of approximately 2 degrees over 12 μ sec which is a somewhat unusual phenomenon since voltage droops and therefore lagging phase shifts usually characterize long pulse operation. In this case, however, the phase advance is consistent since a rising characteristic was discovered during video tests at low peak power, as noted above. (A rising pulse voltage and advancing phase characteristic at low peak power is a desirable feature for low gradient linacs since it enables the bunch to be located slightly ahead of crest at entry to the waveguide, thereby providing compensation against space charge energy spread contributions while minimizing additional phase slippage due to reactive effects).

Figure 7(b) shows the results of an RF phase measurement made across the driver klystron only, to determine its contribution to the total phase variation of the RF output shown in Figure 7(a). This measurement indicated that the drive signal RF phase variation was maintained within a $\frac{1}{4}$ degree bin over a 33 μ sec pulse length and was substantially in agreement with earlier data obtained under laboratory conditions.

A notable feature of the high power RF output pulses, regardless of peak power level or pulse length, was the absence of phase ripple of the type commonly observed with klystrons that are driven by line type modulators and pulse transformers. The high level of video pick-up encountered during the tests required careful shielding and grounding of the monitoring and diagnostic equipment and limited the RF phase bridge to relatively low gain operation. Work is currently in progress to improve the shielding and filtration of the RF phase bridge circuits to allow operation at maximum sensitivity in the video noise environment.

Beam Break-up

The microwave design characteristics and electron beam specifications of the accelerator waveguides are listed in an earlier section of this report, and the layout configuration is shown in Figure 1. With the exception of the buncher section, each waveguide contains eleven uniform, $2\pi/3$ mode segments interconnected by transition regions of progressively increasing impedance. The MIT linac specification of 60 kW of beam power at 400 MeV and 1.8 percent duty requires the demonstration of a peak current of 8.4 mA with pulse lengths extending out to 14 or 15 μ sec. Under the conditions of weak focusing intended for the initial phase of the MIT linac, an extrapolation made in 1966 based on the SLAC experience⁵ suggested that a cumulative beam break-up threshold value of approximately 5 mA could be expected. As a consequence, several microwave design approaches were investigated with the aim of elevating the threshold value to a safe level. A design value of 50 mA was chosen as a goal since the low gradient waveguides at the end of the machine (four sections per klystron) have an i_m value of 60 mA when the klystron is operated at the specified maximum RF peak power of 4 MW. Since, for a given field gradient and charge per pulse, the cumulative type of beam break-up is strongly dependent on the number of identical resonant elements which can interact with the beam and on the HEM_{11} transverse shunt impedance, the investigations¹¹ were concentrated on means of reducing the coherency lengths and on HEM_{11} Q-spoiling techniques.

The design finally adopted for the MIT linac made use of a progressive stop-band concept which required a specific relationship between different waveguide sections along the beam centerline. The eighteen long waveguide sections are comprised of four design groups, A through D, which are similar in external physical detail but differ in microwave design.

The HEM_{11} dispersion characteristics for the group A waveguides are arranged so that the narrow bands of closely spaced undesirable resonances associated with the input coupler and several of the adjoining uniform impedance segments, in the vicinity of the $v_p=c$ intercept, are displaced outside and below the HEM_{11} pass bands of all subsequently located structures, regardless of group affiliation. Similarly, the range of HEM_{11} resonances associated with the critical initial regions of the group B waveguides are designed to fall below the HEM_{11} pass band regions of all following waveguides in groups C and D. This stop-band procedure is applied progressively along the full length of the accelerator. In this manner, the displacement modulation information carried by the beam at low HEM_{11} frequencies, due to transverse fields in the initial segments of waveguides in an upstream group, is excluded from interacting with downstream waveguides; and further deflection amplification at these frequencies is avoided. When using disc loaded waveguides of conven-

tional construction, this technique requires that the iris diameters in the initial region of waveguides in a given group be smaller than those in any preceding group but larger than those in subsequently located groups. This progressive stopband concept is illustrated diagrammatically in Figure 8. Curves A_1 , B_1 , C_1 , and D_1 represents the HEM_{11} ω - β diagrams for the input coupler and the first uniform impedance segment of the waveguides in groups A, B, C, and D, respectively. Similarly, the dashed curves A_2 through D_2 and A_3 through D_3 refer to the second and third uniform impedance segments, respectively. The curves show that undesirable resonances in the proximity of the $v_p=c$ intercept are located below cut-off for the pass band of any following group and that these resonances are separated by approximately 30 MHz from those corresponding segments in the waveguides of neighboring groups.

The measured HEM_{11} resonances and field patterns for each of the 11 uniform segments of the prototype long waveguide, as obtained by excitation and detection through the cavity pumpout holes and RF couplers, were found to agree closely with the computed design data. (The maximum frequency discrepancy was -1.4 MHz at 3946.6 MHz, and this was associated with the first uniform section which contains an off-set coupler and large iris discs. In all probability this discrepancy is due to inaccurately estimating the exact HEM_{11} terminal phase shift through the off-set coupler cavity). Figure 9 is a view of the prototype long waveguide section, after final nodal tuning, undergoing probe tests to evaluate the HEM_{11} resonance and polarization characteristics.

In regard to the latter, it should be noted that during the normal nodal tuning procedure, the cavities were deformed in a specific orientation to provide a simple means of Q-spoiling the HEM_{11} mode. With this technique, a normally large VSWR, due to the mismatch presented by the RF couplers at the higher frequency, is reduced by coupling the HEM_{11} mode into the external system. Individual cavities are tuned (permanently deformed) in a radial plane at 45° to the plane of the rectangular waveguide feed; and for a given set of cavities, the deformation is applied in only one plane, i.e., the cavities of a given segment contain only two wall perturbations, and these are diametrically opposed. In this manner, partial coupling can be obtained for either of the orthogonal planes of polarization, and this results in a lowering of the HEM_{11} loaded Q values and peak field strengths. As an example, the prototype long waveguide had input coupler VSWR maximum values of 2.9 and 2.2 for the two orthogonal HEM_{11} modes at their respective dominant frequencies. The corresponding range of VSWR values for the output coupler extended from 2.2 down to the surprising low value of 1.14.

The second waveguide shown in the background of Figure 9 is used as a very sensitive phase reference in a system which automatically provides frequency correction³ and tracking during the nodal tuning

of production waveguides, regardless of variations in air pressure, temperature or relative humidity.

Injector Linac

Traditionally, the injection and RF systems have always played key roles in the ultimate limitation of beam spectra achieved with conventional microwave accelerators. Now, however, with high duty factor operation, and with the advent of transmitters capable of demonstrating high quality video pulses (<0.1 percent droop and ripple) combined with phase stable RF drive systems, and even greater dependence must be placed on the injector if the inherent resolution of the linac system is to be fully realized. High stability of peak current is no longer as important an issue, owing to the low beam loading conditions and injected peak currents of reduced absolute value, and achieving large fractions of current in 1/10 percent energy bins is now primarily dependent on the attainment of bunches of narrow phase width and good phase stability.

The strong recommendations made here for a 1 or 2 degree bunch width, to improve beam spectra, are clearly not justifiable on the basis of direct contributions to energy spread alone, since a 5 degree bunch **continuously** located on crest (with negligible space charge forces) is equivalent to a 1/10 percent spread in beam energy. (From small angle approximation, $\Delta V/V^0|_0 \approx -(\Delta\theta^\circ)^2/260$). In practical reality, however, with high power RF operation, only after considerable effort is it possible to minimize phase shifts during the pulse, as well as phase drifts from one module to another, to approximately ± 2 degrees. On this basis, and considering the effect of bunch width only, it is apparent that a 5 degree bunch, **if centered**, will time average over an effective 9 degrees of RF, leading to energy spread contributions of $\frac{1}{4}$ percent. With a 1 degree bunch and identical RF conditions, however, the energy spread contribution will remain within a 1/10 percent bin. In practice, these energy dispersion effects are approximately doubled due to nonsynchronous operation and/or non-optimum initial phasing of the bunch at entry to the section. Nevertheless, in conducting an experiment with, say, 1/10 percent analyzing slits, it is clear that the time averaged target current can be increased appreciably as the bunch is reduced from 5 to 1 or 2 degrees.

For the injector linac, the concept chosen as the most likely to meet the bunch objectives, less than 2 degrees of longitudinal phase space for peak currents up to 25 mA at not less than 6 MeV beam energy, was based upon the use of a high potential electron source and two stages of bunch compression, bearing in mind the need to minimize both cost and number of components.

The first stage, designed to operate at beam energies within the range of 300 to 500 keV, utilizes a biased RF chopper prebuncher com-

ination⁶ to compress a 120 degree chopped beam to <10 degrees. A stabilized, gas insulated, HV dc power supply energizes the electron gun assembly which comprises a small indirectly heated cathode, a non-intercepting modulation extraction electrode, and an electrostatic focusing electrode followed by 13 intermediate accelerating electrodes designed for uniform gradient operation. The dc magnetically biased TE₁₀₂ chopper is followed by a slotted buncher cavity and a chopping aperture designed for 10 kW dissipation. A drift length of approximately 130 cm was chosen to limit phase modulation at injection to the buncher waveguide to $<1\frac{1}{2}$ degrees for a gun potential variation of 1/10 percent.

The second stage consists of a 1.2 meter long, 6 MeV disc loaded buncher waveguide, designed to provide approximately 5 to 1 compression of the injected bunch, connected in series to a 3.7 meter waveguide. Apart from the input coupler and several neighboring cavities which have phase velocities slightly less than c, the buncher waveguide is designed as a phase velocity of light, $2\pi/3$ mode circuit. The very high level of dissipation in the short buncher waveguide presented a difficult design problem since brazing cooling tubes directly onto the structure, the technique used for the longer sections, would not prevent dangerously high stresses from developing in the vicinity of the disc apertures. As a design compromise, to avoid the expense of using cooling ducts in the discs, the outer peripheries of the discs were fluted to form a high velocity, multiple channel, cooling jacket system. The buncher waveguide requires a flow of 100 GPM and an automatic temperature-phase control system³ similar to that used for the other waveguide sections. Typical disc and spacer components for the buncher waveguide are shown in Figure 10, together with some of the electron gun components including the cathode assembly and several focusing electrodes.

Linac Facility at Middleton, Massachusetts

A layout of the overall facility including the control and experimental areas is shown in Figure 11, and Figure 12 shows a view of the building construction nearing completion at the Middleton site, which is located 20 miles north of Boston. A brief summary of the construction schedule is listed below.

Building Design Completed	July 1967
Building construction contracted	Oct. 1967
Partial occupancy	July 1969
Full occupancy and completion of utilities (schedule)	Jan. 1970
Electrical Utilities, Water and Vac System Design Concept	Aug. 1967
Completion of electrical and water utilities (schedule)	Jan. 1970

Transmitters Contracted	March 1967
Prototype transmitter: First RF tests	June 1969
Master Driver Design Concept	Jan. 1968
Completion of engineering design	Sept. 1968
Completion of master driver unit	Feb. 1969
Overall Drive System Design Concept	Sept. 1967
Completion of engineering design	Aug. 1969
Accelerator Waveguides Design Concept	Dec. 1966
Completion detailed engineering microwave design	Dec. 1967
Waveguide construction contracted	Feb. 1968
Completion of overall engineering design	Aug. 1968
Completion of prototype long waveguide	April 1969
Commence installation of accelerator waveguides (schedule)	Jan. 1970
Completion of injection Linac Design Concept	April 1968
Completion of prototype HV electron gun	Sept. 1969
Beam Switch Yard Design Concept	Jan. 1967
Completion of engineering design (schedule)	Sept. 1969
Energy Loss Spectrometer Design Concept	Jan. 1967
Completion of engineering design (schedule)	Sept. 1969

Acknowledgement

The author acknowledges the fine supporting efforts of a team of less than 40 MIT technicians, engineers and physicists, working under the restrictions of a very limited budget, to design and construct a relatively large facility. The cooperative efforts and diligence of our various contractors in the production manufacturing and testing of the major sub-systems, are also gratefully acknowledged.

REFERENCES

1. E. A. Knapp, "Resonantly Coupled Standing Wave Accelerator Structures for Electron and Proton Linac Applications", *IEEE Trans. Nucl. Sci.* NS-16, No 3, June 1969, 329.
2. H. Leboutet, G. Azam, F. Netter and C. Tzara, "First Operation of the High Duty Cycle Saclay Electron Linac (ALS)", *IEEE Trans. Nucl. Sci.* NS-16, No 3, June 1969, 299.
3. J. Haimson, "High Duty Factor Electron Linear Accelerators", Chapter 3.2, *Linear Accelerators*, P. Lapostolle and A. Septier, (Eds.) (North-Holland Publishing Co., Amsterdam, 1969).

4. J. Weaver and R. Alvarez, IEEE Trans. MTT, MTT-14, № 12, Dec. 1966, 623.
5. R. B. Neal and W. K. H. Panofsky, Science 152, 1966, 1353.
6. J. Haimson, IEEE Trans. Nucl. Sci. NS-12, № 3, June 1965, 499.

ДИСКУССИЯ

Зыков: Какого типа секция в вашем ускорителе с постоянным импедансом или с постоянным градиентом?

Haimson: Each waveguide section consists of 11 subsections each of constant but different impedance. The subsections are joined together by means of matched transitions.

Чижов: Не могли бы Вы высказать свое мнение о возможности создания линейного электронного ускорителя на энергию 400 MeV с коэффициентом заполнения 10% и более?

Haimson: When you go to linacs with duty factors more than 10% you will meet immediately serious economical difficulties. There are klystrons with average power up to 80 kW now, and one may expect that we shall have soon klystrons with average power up to 150 kW now. If we take such klystrons and duty factor 20% then the peak power of a RF source will be of order of a few MW. and we shall be forced to use very long waveguides with high attenuation in order to get required energy of electrons. Such waveguides have several drawbacks, namely, very rapid decrease of energy gradient. Surely linacs with energies of 400--500 MeV may have duty factor up to 4%, linacs with energies 150--300 MeV to 10%. However further increase of the duty factor is not worthwhile from the economical point of view.

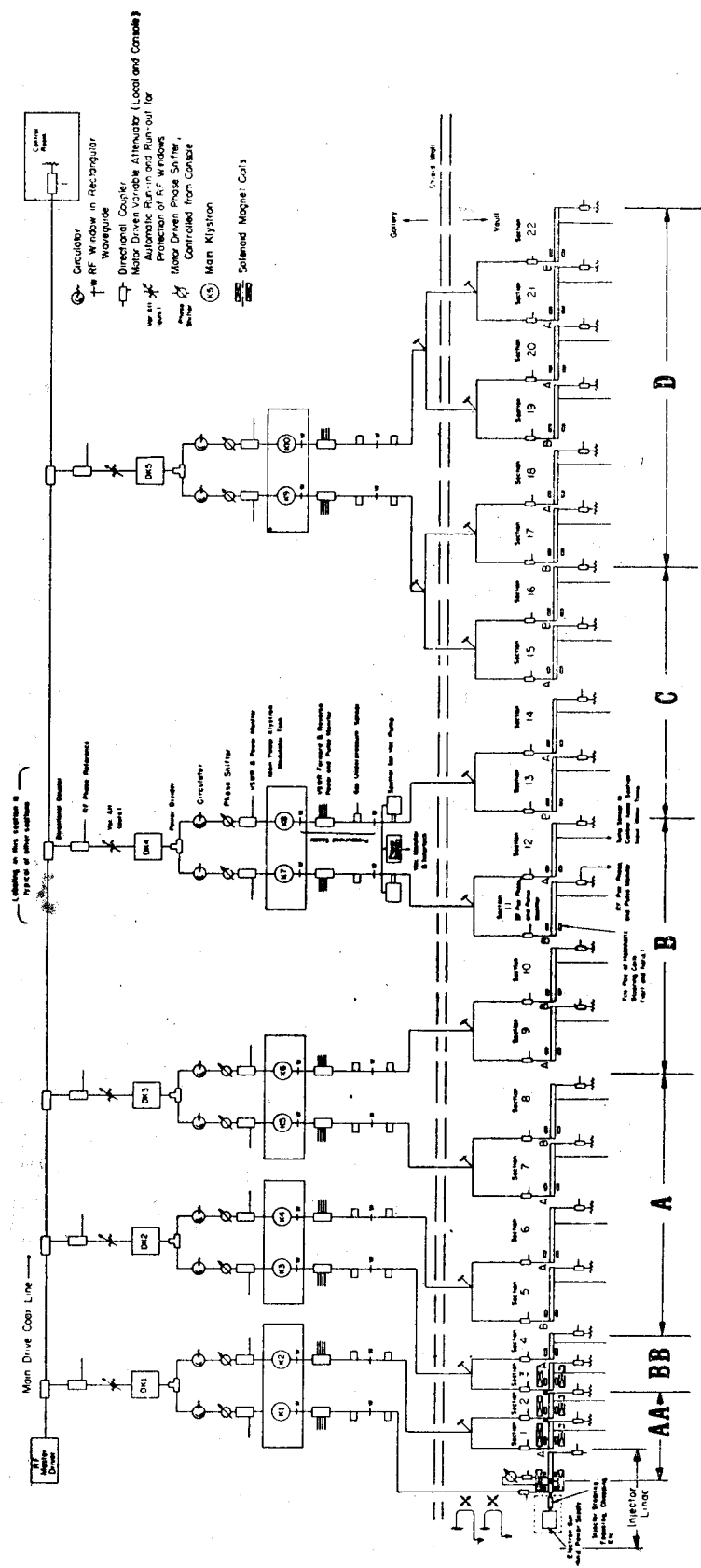


Fig. 1.

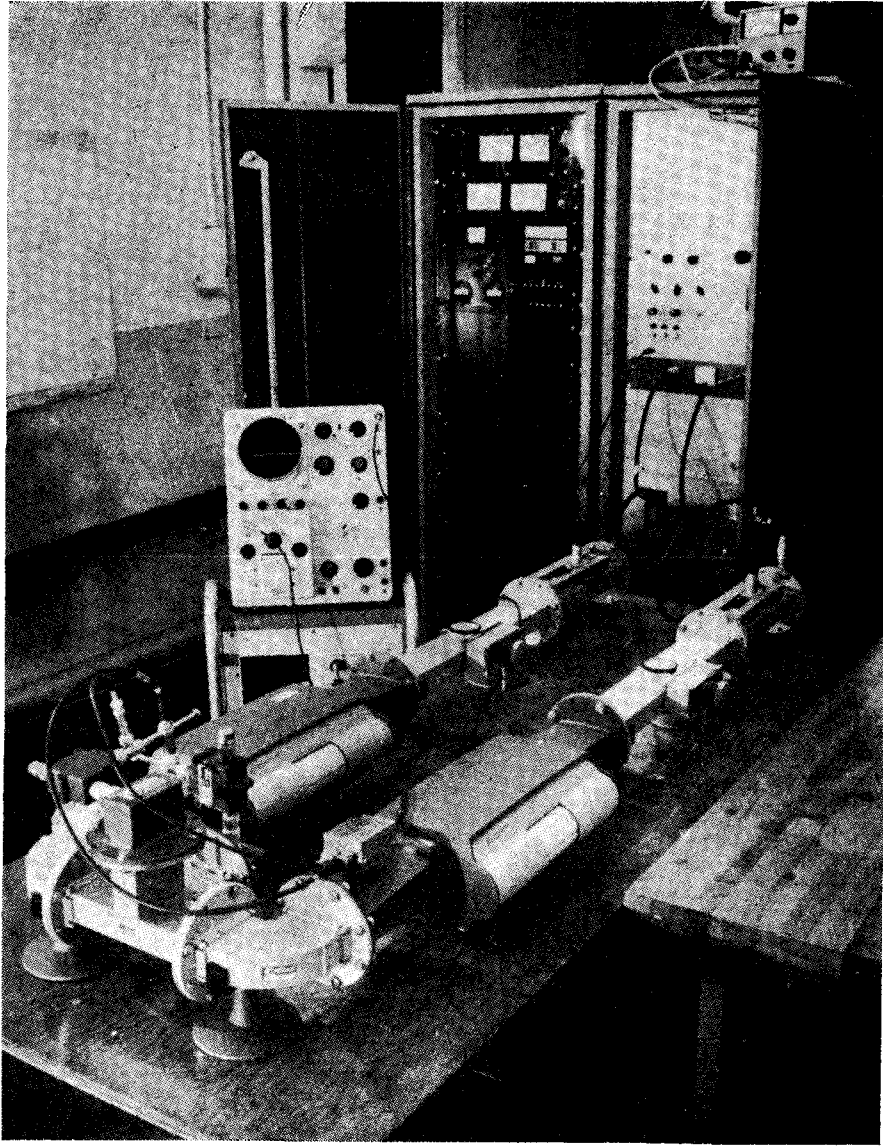


Fig. 2.

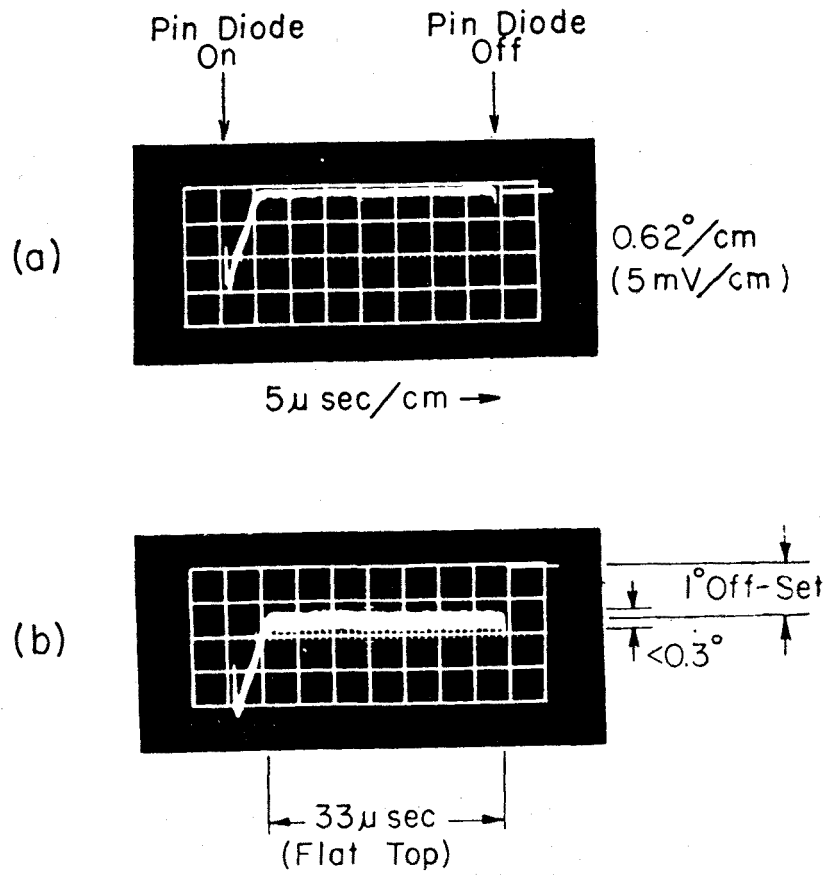


Fig. 3.

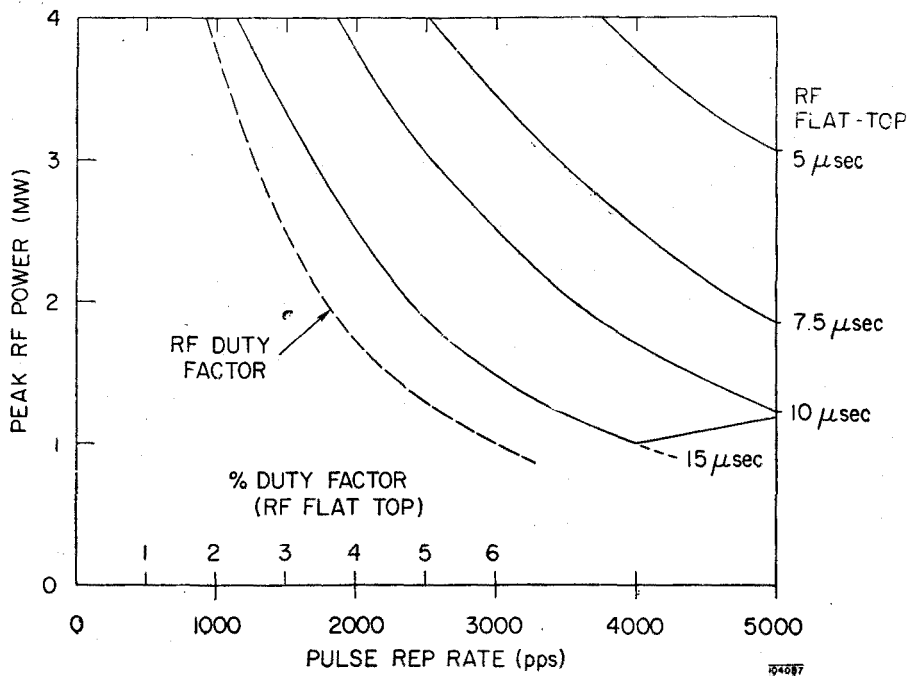


Fig. 4.

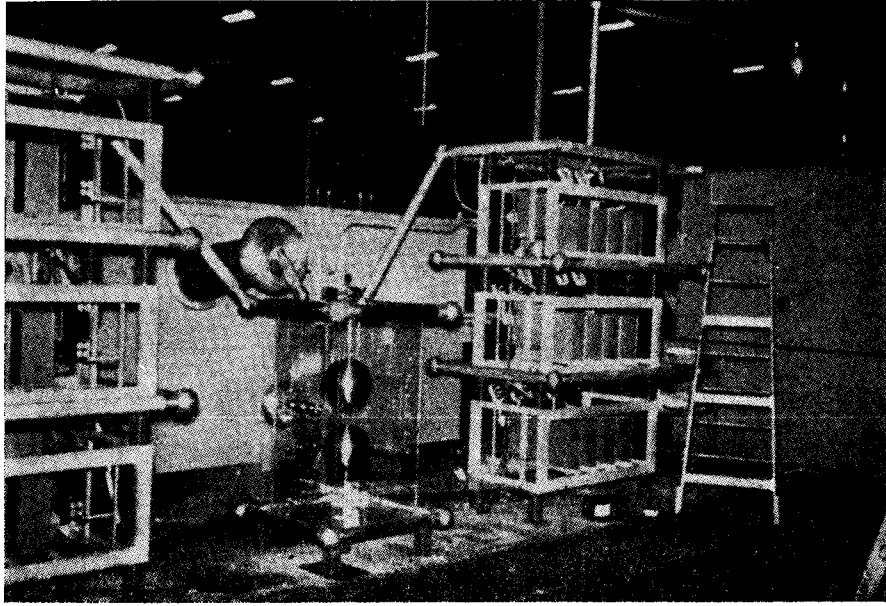


Fig. 5.

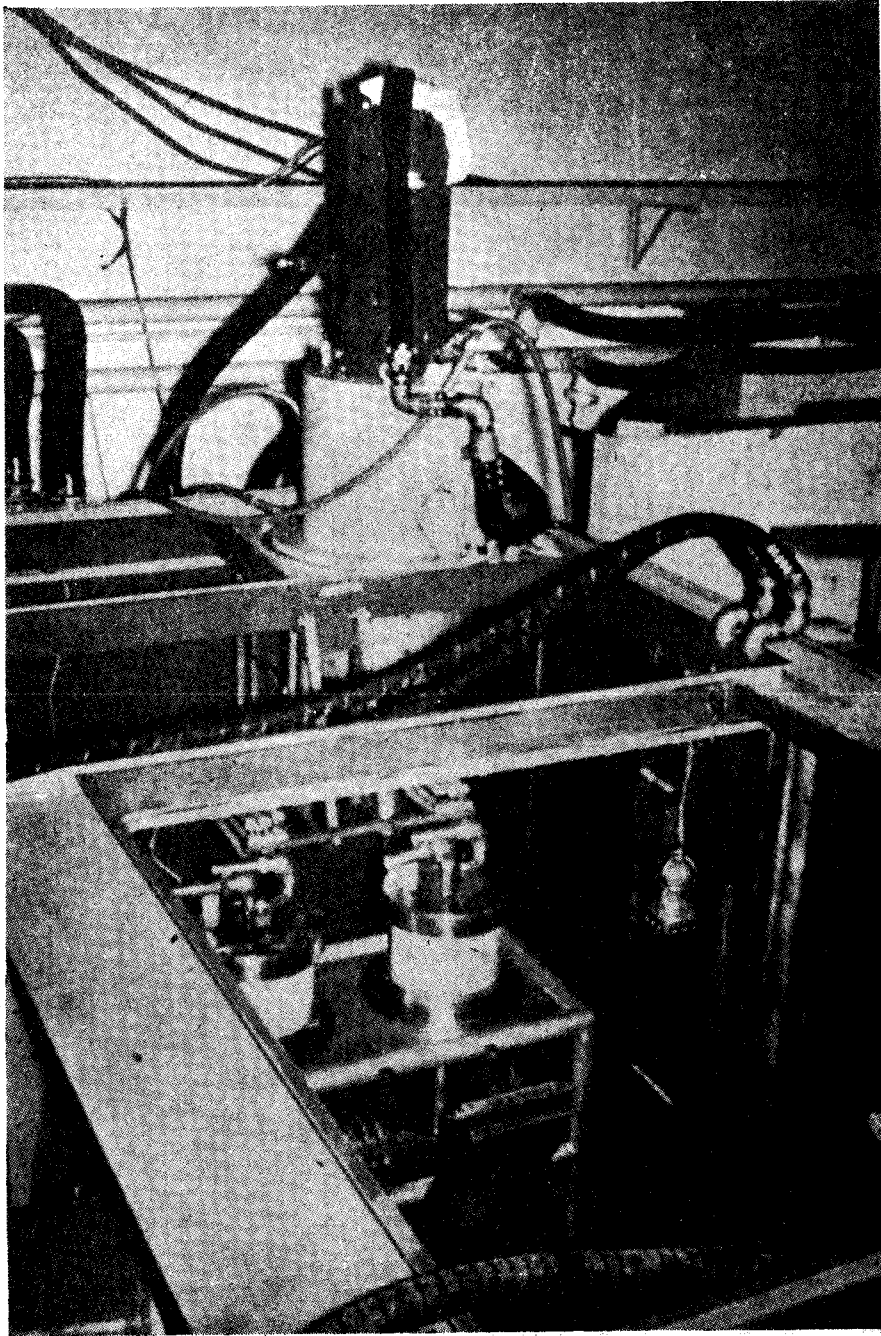


Fig. 6.

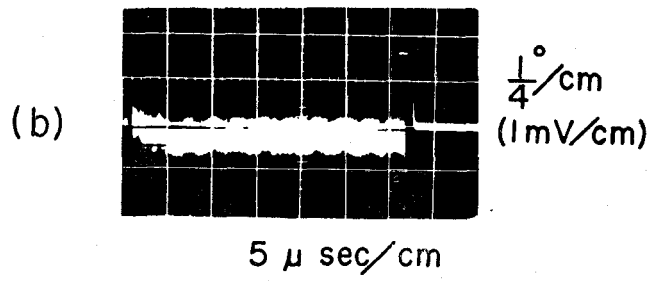
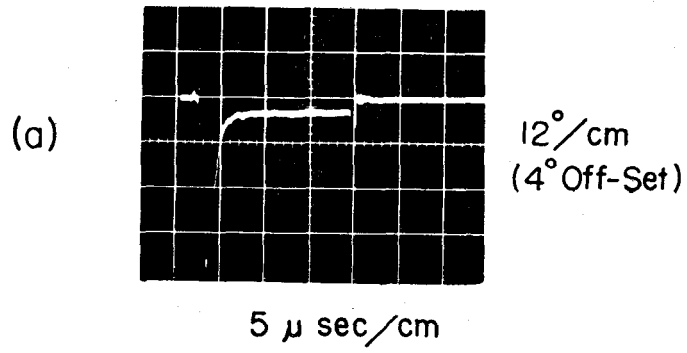


Fig. 7.

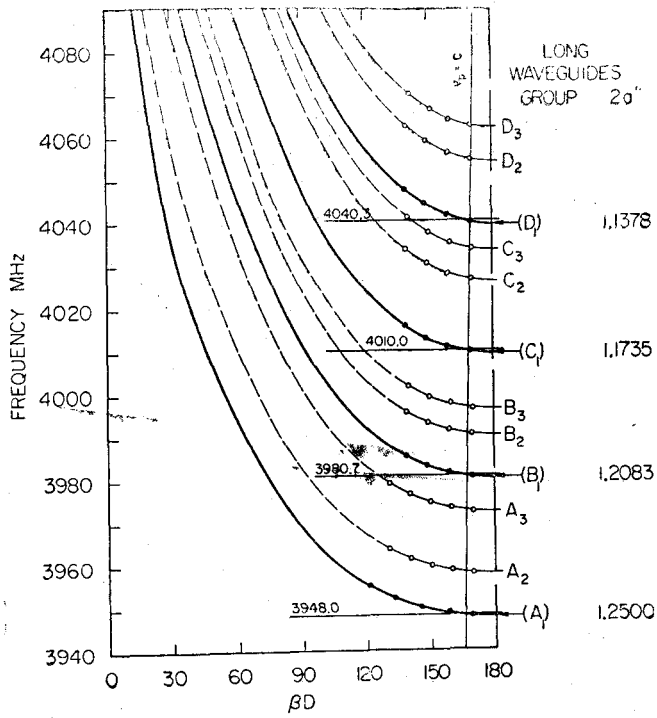


Fig. 8.

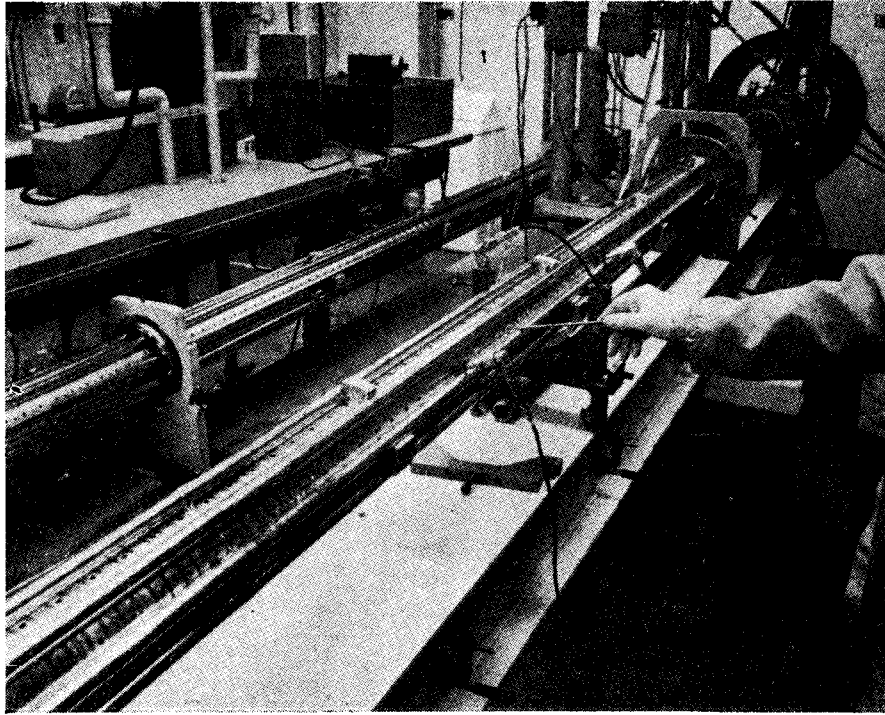


Fig. 9.

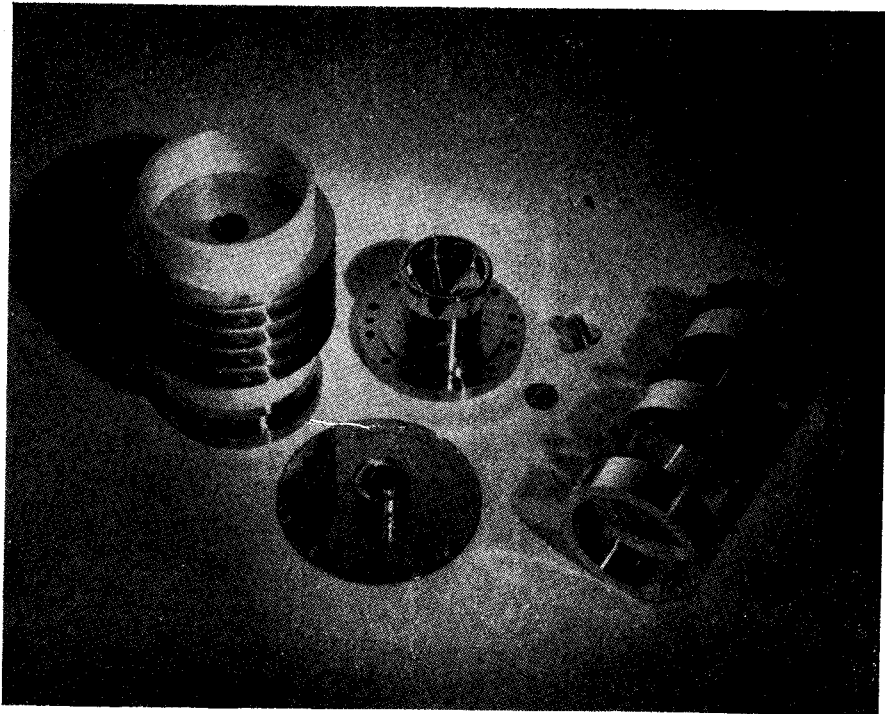
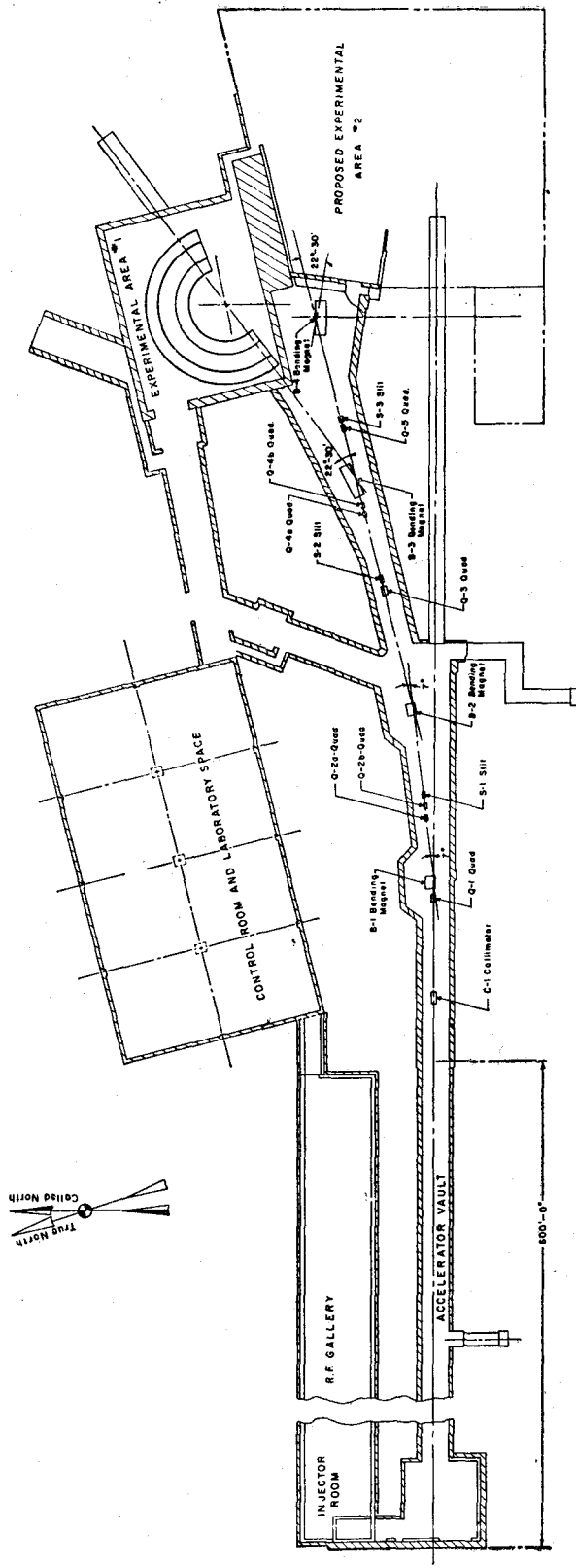


Fig. 10.



Scale Feet

Fig. 11.

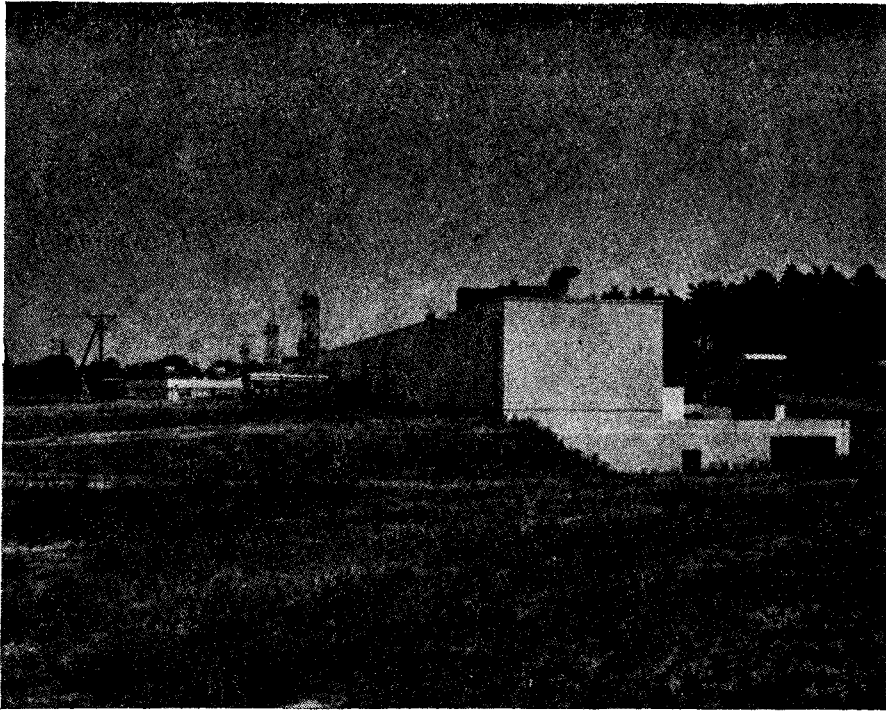


Fig. 12.